Anti-Biofouling, Thermal, and Electrical Performance of Nanocomposite Coating with Multiwall Carbon Nanotube and Polytetrafluoroethylene-Blended Polyphenylenesulfide

EUNSOO YANG

Active Materials and Processing Laboratory, Department of Mechanical Engineering, University of Nevada, Reno, 664 North Virginia Street, Reno, NV, 89557 USA

TAESEON HWANG, ANUPAM KUMAR, KWANG J. KIM

Active Materials and Smart Living Laboratory, Department of Mechanical Engineering, University of Nevada, Las Vega, 4505 South Maryland Parkway, Las Vegas, NV, 89154 USA

Correspondence to: Kwang J. Kim; e-mail: kwang.kim@unlv.edu.

Received: November 17, 2015
Accepted: May 19, 2016

ABSTRACT: Corrosion, erosion, and fouling by scale deposition are detrimental to heat-exchanger tube at geothermal binary-cycle power plants. In this work, polytetrafluoroethylene was blended in a polyphenylenesulfide matrix with different concentrations of multiwall carbon nanotube (MWNT) using the melt-mixed method to reduce scale deposition on the metal surface. The prepared nanocomposites with different concentrations of MWNT were characterized by various properties such as morphology, hydrophobicity, electrical, thermal, and rheological properties. The morphology of nanocomposite was changed from smooth to nano-pin-like with the addition of MWNT. The varied concentration of MWNT led to differing hydrophobicity of nanocomposite. Increasing the loaded amount of MWNT in the nanocomposite led to decreased electrical resistivity up to 3.1×10^3 Ω cm because of percolation of the MWNT in the polymer matrix. In addition, we investigated the enhancement of thermal performance (10% of lower crystallization peak) of the prepared nanocomposite. These performance results indicate that the prepared nanocomposite can be widely adopted for use in high-performance heat exchangers in geothermal industries. © 2016 Wiley Periodicals, Inc. Adv Polym Technol 2018, 37, 21728; View this article online at wileyonlinelibrary.com. DOI 10.1002/adv.21728

KEY WORDS: Anti-biofouling, Carbon nanotube, Geothermal, Nanocomposites, Polytetrafluoroethylene

Introduction

Corrosion, erosion, and fouling by scale deposition are the critical issues in using heat-exchanger tube at power plants which act as an insulator and increase the transfer resistance. In general, heat exchanger and its major components consist of expensive materials such as, nickel alloys, titanium alloys, or stainless steel. In particular, bio-fouling on the metal surface of heat exchangers make problem on cleaning and maintenance which is due to the usage of seawater as coolants.[1] Therefore, the anti-fouling surface in heat exchanger could be important to reduce the operation cost and sustain the performance. An effective and desirable approach is surface modification of the equipment to make it less attractive for the bio-fouling components.[2] The protection and modification of these high-cost metal surfaces against environmental attack is usually achieved by using an adherent and protective coating deposited onto the metal surface.

Polytetrafluoroethylene (PTFE)[3–5] has been widely used as coating materials on the metal surface to provide excellent chemical resistance, high-temperature stability, and nonsticking properties. Although PTFE has demonstrated good surface modification, there are inherent drawbacks which limit its practical applications, such as poor thermal conductivity, poor abrasion resistance, and poor adhesion to the metal substrate.[3] In addition, polyphenylenesulfide (PPS) has attracted considerable interest as an engineering plastic because of its good thermal stability, high-temperature stability, inherent flame resistance, good chemical resistance, and excellent friction properties.[6] However, the applications of pristine PPS have been somewhat limited with relatively low glass-transition temperature (T_g) compared to its high melting temperature, brittleness, and low strength. Thus, its applications in geothermal plants which require harsh environmental conditions, was previously suggested by T. Sugama.[3–5]

In addition, carbon nanotube (CNT) has attracted increasing research interest due to their desirable properties, such as a

high aspect ratio and excellent thermal, electrical, and mechanical properties.[7,8] In particular, CNT have been widely used in water pollution industries, such as absorption of pollutants,[9] chromium removal,[10] and lead removal.[11,12] However, CNT is strongly affected by van der Waals' attraction, which affect aggregation of CNT.[13] This makes it difficult to disperse CNT in polymer matrix, resulting in a decrease in their mechanical and electro-conductive properties. Therefore, there are important points to explore more elaborately: (i) the reinforcing potential of CNT and (ii) how to enhance the properties of a polymer matrix in order to ensure a uniform dispersion, exfoliation, and orientation of CNT. Meanwhile, improving the interaction between CNT and a polymer matrix is also important.[14] Thus, previous studies have reported that polymers containing an aromatic ring with hydrophobic properties, such as polystyrene, could have a strong interaction with CNT through π–π stacking.[15] PPS contains a benzene ring on its backbone. Therefore, a substantial interaction between PPS and CNT is able to expect due to π–π stacking, which makes the examination of PPS/CNT composites feasible.[16] Melt compounding process between polymer and CNT is widely adapted to fabricate polymer nanocomposite.[17] In this process, polyethylene glycol (PEG) as a binder is incorporated with the melted compound to reduce less uniform pores and cracks by high-temperature sintering, which causes further damage to the corrosion resistant property at the substrate interface.[18]

This work reports the results regarding the preparation, surface properties, electrical properties, and mechanical properties of a multi-micro-nanostructure of PTFE-blended PPS nanocomposite with multi-walled carbon nanotube (MWNT). The nanostructured morphology of the resulting composites was investigated using a scanning electron microscope (SEM). Their general mechanical properties were studied by dynamic material analyzer (DMA). In addition, rheological and crystallization behavior of composites were investigated to study the multi-micro-nanostructure of composites with varied concentrations of MWNT. Acid-treated MWNT was shown good dispersibility in the polymer matrix and also reasonable interaction with PPS, resulting in a great improvement of electrical and mechanical properties of the composites. In addition, the resultant nanoporous network has an entire polymer coated onto the CNT surface with more uniform porosity and lower cracks in the multi-micro-nanostructure. The induced structural effects on multi-micro-nanostructures can be formed a hydrophobic surface through roughness of surface and its low surface energy (with PTFE). These methods are mainly based on the approaches that make a modified rough surface with a hydrophobic material of low surface energy. This work provides a simple and fast way to prepare PTFE-blended PPS with MWNT composites with excellent properties, with an expectation of a wider application of PTFE-blended PPS with MWNT nanocomposites for use in high-performance heat exchangers in geothermal industries.

Experimental

MATERIAL

PTFE-blended PPS was produced by simple melt-mixed method at different concentration of MWNT, using a nonionic surfactant, PEG, as the structure-directing template.[19] PTFE, PPS, PEG, MWNT, and nitric acid used in this work were purchased from Sigma-Aldrich (St. Louis, MO, USA). MWNT were used as received, without any pretreatment. PPS used in this work was purchased in powder type.

COMPOSITE FABRICATION

Uniformly distributed MWCNT within the polymer coating was produced by the oxidation of CNT by means of immersion in nitric acid at room temperature. After oxidation process, the carboxyl and hydroxyl groups would be formed on the CNT surface. The CNT was dispersed effectively because of the repulsion between these negatively charged groups, and the solution remained stable for over 2 weeks. Coating was carried out using PEG as a nonsurfactant after the solution was prepared. To prepare the composite samples, PPS powder and PTFE particles were blended with PPS (in the weight ratio of 3:2). Then, it was mixed with CNT and PEG in an isopropanol solution on the hotplate at 300°C. The resulting mixtures were applied to brass surfaces, and baked in an oven at a temperature of 340°C for 4 h.

CHARACTERIZATIONS

PTFE-blended PPS with PEG coatings having varied concentration of MWNT on brass tube was obtained and their surface morphology was investigated by SEM (Mini-SEM, EVEX). The samples were sputter-coated with platinum. The water contact angles were measured by a contact angle analyzer (CAM 100; KSV Instruments Ltd., Helsinki, Finland). The water droplet used for the measurement was 5–15 μL in volume. The thermal properties of nanocomposites were investigated with a differential scanning calorimeter (DSC, TA 5000; TA Instruments, New Castle, DE, USA). The heating rate was 5°C/min for the DSC. All experiments were run under a nitrogen purge. The electrical resistance of nanocomposites was measured with inter-digitated electrodes by two probe methods. Resistivity of nanocomposites was calculated by measuring the resistance values, area, and thicknesses of specimens. The area and thickness of samples were measured with a vernier caliper (ABSOLUTE; Mitutoyo Co., Kawasaki, Japan). To characterize the mechanical properties of the prepared composite samples, the DMA experiment was carried out using a Pyris Diamond DMA (Perkin-Elmer, Waltham, MA, USA). with analysis program (Seiko Instruments Inc., Chiba, Japan). The DMA frequency range was from 0.01 to 100 Hz and was performed at room temperature.

Results and Discussions

MORPHOLOGICAL CHANGES WITH INCREASING MWNT CONTENT AND THE EFFECT OF PEG ON MORPHOLOGY

Figure 1a shows the surface morphology of the acid-treated MWNT. There was no damage or cutting on the nanotubes under oxidation treatment using nitric acid.[20,21] A cross-section of the polymer matrix with MWNT and PEG is shown in

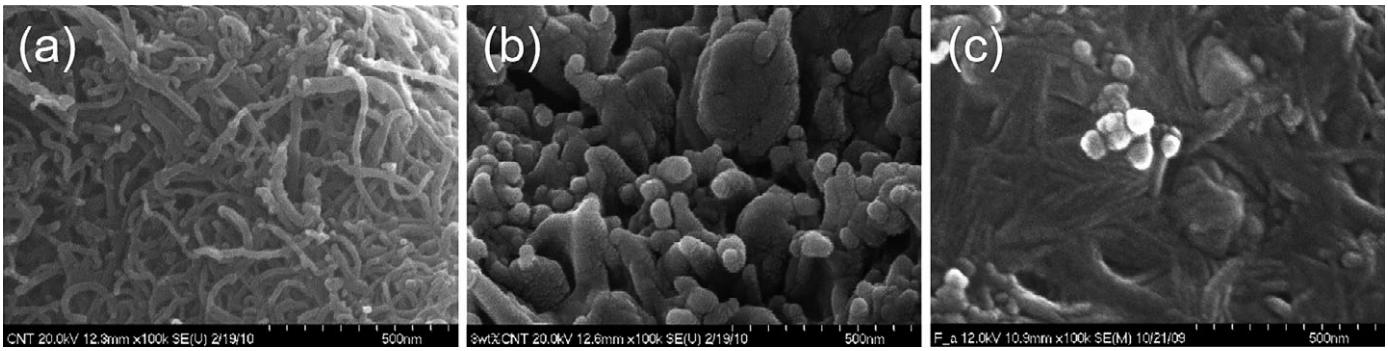

FIGURE 1. (a) the surface morphology of the acid-treated MWNT, (b) cross-section image (SEM) of the encapsulated MWNT with a PTFE-blended PPS polymer matrix and with the nonionic surfactant as PEG, and (c) without PEG.

Fig. 1b. The SEM images show that the MWNT were encapsulated with polymeric materials and linked with other CNT by means of the PTFE-blended PPS polymer matrix, which maintained the optical and chemical stability of the deposited film. The counterpart polymers were homogeneously coated on the surface of the MWNT in the PEG-mixed polymer matrix by a melt-mixed method. The nanocomposites without PEG showed only a dense packed morphology or irregular polymer particles in spite of a mixed MWNT of 3 wt% in the polymer matrix, as shown in Fig. 1c. This demonstrates that the use of a surfactant in the experiments, that is, PEG was indispensable to the morphologies of the final products.

Figure 2 shows the surface morphologies of the PTFE-blended PPS with/without a PEG coating having various MWNT concentrations on brass tube. The PTFE-blended PPS typically shows a smooth surface morphology, as shown in Fig. 2a. However, by adding small amount of MWNT, the phase morphology changes from a smooth surface to a nano-pin-like structure, as shown in Figs. 2b and 2c. The content of MWNT was 3 and 5 wt%, respectively. In comparison, SEM images of the sample without PEG revealed a smooth surface and irregular sheet-structured morphology or embedded nanoparticles (Figs. 2d–2f). However, such a smooth surface is believed to be an inherent characteristic of blended PPS surfaces (Fig. 2d). The key to understand the change in phase morphology by adding PEG is to know its mechanism in the blended system. As it has already been noted in the experimental section, PTFE-blended PPS with MWNT was synthesized by a melt-mixed method at various MWNT concentrations using PEG as the structure-directing template.[19] As for the growth mechanism of PPS with MWNT compounds, the role of the surfactants should be taken into

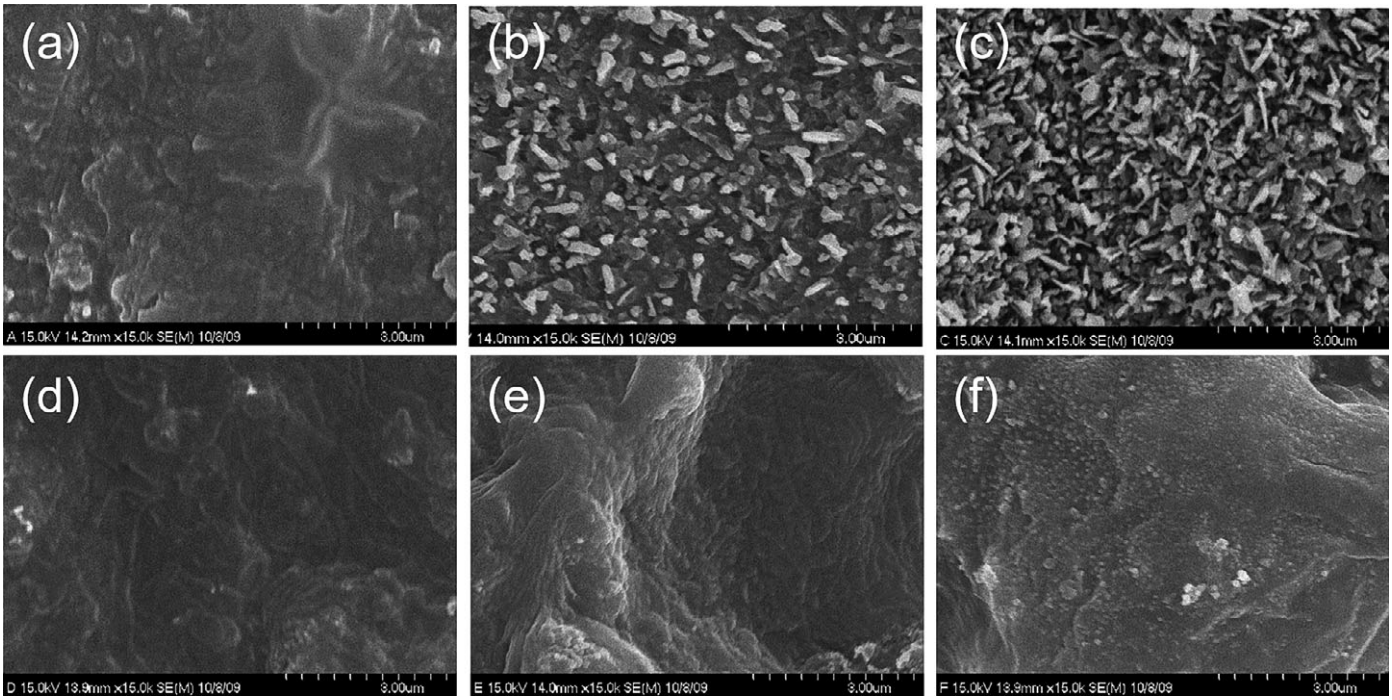

FIGURE 2. SEM images of PTFE-blended PPS films prepared with PEG and with a MWNT content of (a) 0, (b) 3, and (c) 5 wt%; without PEG and with MWNT content of (d) 0, (e) 3, and (f) 5 wt%.

consideration. PEG is a sort of nonionic surfactant.[22] Its monomer was apt to exist with chain structures in solution, which made it possible for PPS with MWNT compounds to grow along the chain direction. The chain structure of the PEG induced the PPS with MWNT compounds to grow into quasi-1D nanostructures to a certain extent.[23]

SURFACE MODIFICATION INDUCED HYDROPHOBICITY

Sun et al [24] proposed the following equation to describe the contact angle θ of a rough surface by considering the increase in the practical surface area:

$$\cos\theta' = \frac{r(\gamma_{SV} - \gamma_{SL})}{\gamma_{LV}} = \gamma\cos\theta \quad (1)$$

Figure 3 shows the results of water contact angle of prepared specimens. Pristine PPS and PTFE show 80 and 103° of water contact angle value, respectively (shown in Figs. 3a and 3b). Figure 3c shows PTFE-blended PPS without MWNT, and the water contact angle is 131°. When MWNT is added in PTFE-blended PPS with 3 and 5 wt%, water contact angle is increased to 169 and 171°, respectively (shown in Figs. 3d and 3e). Based on the SEM micrographs in Fig. 2, the difference of hydrophobicity between Figs. 3c–3e is attributable to the rough structure owing to the surface coating of polymers on functionalized MWNT that were PEG-based. Therefore, Figs. 3c–3e are composed of different roughness, which were large and induced by primary MWNT. Building on the theory of wetting of rough surfaces, unique surfaces were developed in this study that were chemically hydrophobic with multi-micro-nanostructures, that is, the droplet was in contact with a hydrophobic material and exhibited super-hydrophobic properties (high contact angle, $\theta > 150°$).

The decrease in the contact angle was an indicator of loss of both hydrophobicity and trap air that are often found in nanostructured and/or micro-structured material. This multi-level roughness contributes directly to super-hydrophobic surfaces, suggestive of micro- and nanoscale roughness and to the control of fouling, as described in the following section.[25] In addition, there could be a contribution from constituents. It is our belief that PTFE and MWNT are major contributors to affect the wetting property of the composite samples. When super-hydrophobic surfaces are immersed, air bubbles are entrapped into micro- and nanosized pores at the solid surface, and a mix of solid–liquid and solid–gas interfaces is created.[26] The extent of solid–gas interface is proportional to the degree of hydrophobicity of the material. The higher the hydrophobicity, the larger the solid–gas interface will be. The air bubble layer creates a barrier that may prevent adsorption of micro-organisms in the short term. During early stages of immersion, air bubbles occupy most of the surface. However, the resistance of that layer to micro-organisms will depend on the design of air adsorption sites. Loss of super-hydrophobicity occurs in a variety of ways. One way is that air may be dissolved in water for long-term submersion. More importantly, it occurs when the chemistry or structure of surface is changed due to the attachment of a conditioning layer of macromolecules. Therefore, the non-wetting property of a surface is the indicator of cleanliness in this instance.

THERMAL PROPERTIES

DSC was employed to evaluate the effect of MWNT on the crystallization and melting behavior of different types of PTFE-blended PPS with MWNT composites, as depicted in Fig. 4. Table I lists the measured endothermic energies, ΔH_{m1} and ΔH_{m2}, generated at the melting points of PPS and PTFE, and the exothermic crystallization energies, ΔH_{c1} and ΔH_{c2}, of PPS and PTFE for the coating systems.

It can be observed from Table I that the crystallization temperature T_c was obtained from the maximum of the

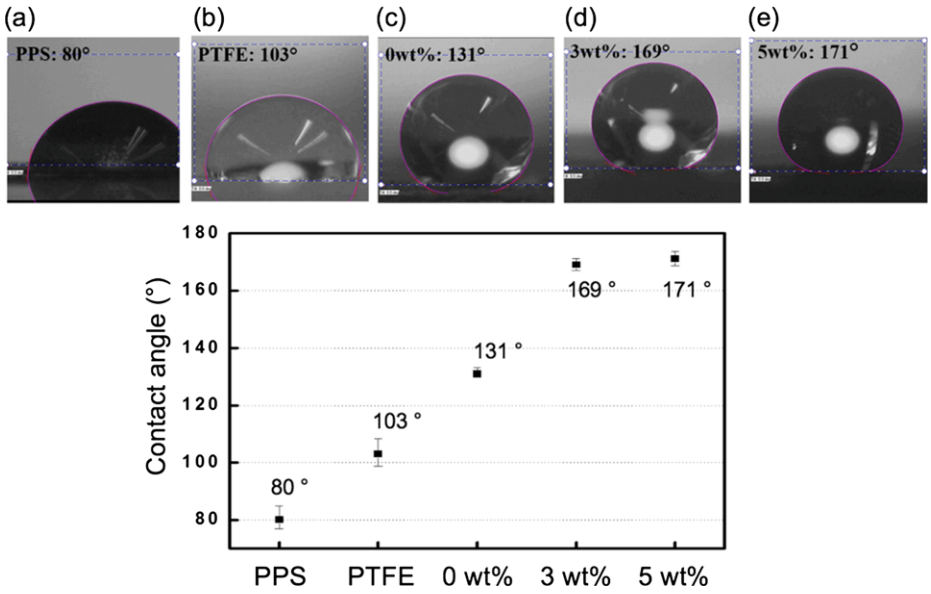

FIGURE 3. The contact angle versus the mass fraction, and photographs of a spherical water droplet on prepared samples: (a) PPS, (b) PTFE, PTFE blended PPS with (c) 0, (d) 3, and (e) 5 wt% of MWNT on carbon stainless steel.

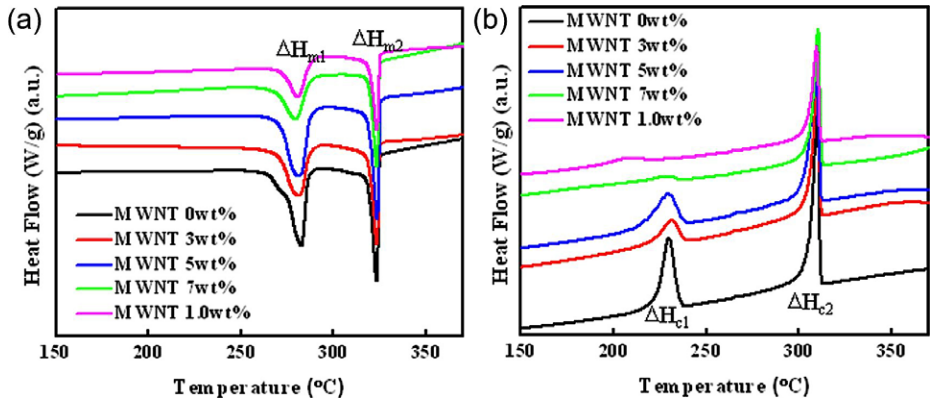

FIGURE 4. Effect of c-MWNT on (a) crystallization and (b) melting temperature of the nanocomposites.

TABLE I
DSC Results for PTFE-Blended PPS with MWNT Nanocomposites at a Cooling Rate of 10°C

	Exothermic crystallization energy (J/g)				Endothermic melting energy (J/g)				Degree of supercooling ($\Delta T = T_m - T_c$)
Coating system	T_{c1} (°C)	ΔH_{c1}	T_{c2} (°C)	ΔH_{c2}	T_{m1} (°C)	ΔH_{m1}	T_{m2} (°C)	ΔH_{m2}	ΔT_1
PTFE-blended PPS	229.59	20.84	309.73	13.97	282.79	16.48	323.52	9.33	53.2
PTFE-blended PPS with 3wt% MWNT	230.99	8.52	309.77	13.26	280.63	12.13	323.63	10.31	49.64
PTFE-blended PPS with 5wt% MWNT	229.03	17.47	308.74	17.08	281.16	16.99	323.73	12.30	52.13
PTFE-blended PPS with 7wt% MWNT	226.80	1.54	310.18	14.60	279.81	9.55	323.61	9.51	53.01
PTFE-blended PPS with 10wt% MWNT	204.54	2.37	309.39	13.58	281.11	10.07	323.77	9.58	76.57

exothermic peak. The crystallization temperature was about 230°C for PPS of pure PTFE-blended PPS without MWNT composites. The incorporation 3–7 wt% of MWNT did not show much change in the crystallization peak. However, there was a progressive shift in the crystallization peak toward a lower temperature at approximately 205°C, and a steep change in the degree of supercooling for the composite with 10 wt% MWNT.

Many researchers [27] have reported that MWNT enhances the nucleation of crystallization for polymer/MWNT nanocomposites. However, it could not effectively act as nucleating agents until a loading 7 wt% of MWNT in the PTFE-blended PPS. The molecules of PPS are rigid compared to conventional polymers, which implies that larger translations of PPS molecules are required for recrystallization in the melt state. In addition, the crystallization of PPS occurs very rapidly on cooling.[28] Therefore, it is suggested that a small amount of MWNT would not act effectively as a nucleating agent because of these properties for crystallization of PPS. In addition, the MWNT network imposed a confinement on polymer chain diffusion and crystal growth, which slowed down the overall crystallization process. This effect is attributed to the interactions between the matrix and the nanoscale filler that occurred during the crystallization process. Therefore, a progressive shift could not occurs until a loading 7 wt% of MWNT in the PTFE-blended PPS in spite of increasing the content of MWNT. However, we observed that 10 wt% of MWNT composite was intriguing since a large amount of MWNT usually acts as a nucleating agent that increases the crystallization rate. This is because nucleation starts simultaneously at multiple centers.

The ΔT remains unchanged from 49.6 to 53.2°C after incorporating 3–7 wt% of MWNT. The lack of change in the crystallization rate indicates that the dispersion of MWNT in the polymer matrix hindered molecular movement in the melt state. In contrast to the degree of crystallinity, the crystallization rate was greatly affected by the addition of large amounts of MWNT. The increase in ΔT was about 77°C after incorporation 10 wt% of MWNT; this could be related that the crystallization rate was reduced by incorporating large amounts of MWNT filler. This explained why the crystallization temperature shifted to lower temperatures with MWNT fraction. It can also be pointed out that there may be a considerable amount of defects causedto the crystal. This needs to be further studied for clarification.

ELECTRICAL CONDUCTIVITY

Figure 5 shows the conductivity change in PTFE-blended PPS with MWNT compounds as a function of MWNT concentration. The electrical resistance decreased with increased MWNT fraction, and exhibited a percolation of MWNT into the polymer matrix. The volume resistivity of pristine PTFE-blended PPS and PTFE-blended PPS with 1 wt% of MWNT was measured 3×10^{16} Ω cm. For the concentrations of MWNT 3, 5, 7, and 10 wt%, the volume resistivity was

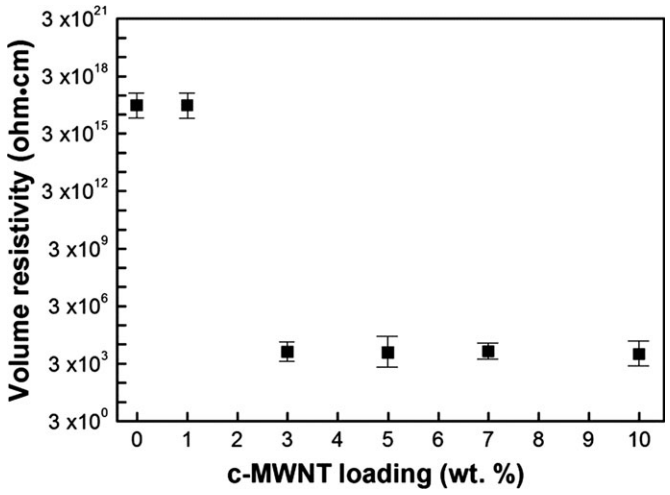

FIGURE 5. Resistivity of the nanocomposites as a function of PTFE-blended PPS with MWNT composite films.

measured 3.9 × 10^3, 3.6 × 10^3, 4.2 × 10^3, and 3.1 × 10^3 Ω cm, respectively. The resistivity of sample would start to reduce from 3 wt% of MWNT in composite. The percolation threshold was expected to be around 3 wt% of the MWNT concentration, deduced by typical percolation behavior into melt-mixed polymer composites. From Fig. 2, it was confirmed that the prepared composite films had a nano-pin structure of composite film and the high percolation threshold results from the homogeneous dispersion of MWNT in a polymer matrix. The conducting network formed in a MWNT-filled polymer was robust and less segregated, with a low aspect ratio of MWNT filler into the polymer matrix. The resistivity did not decrease further with increasing MWNT concentrations because of an increase in aggregation with increasing resistivity of aggregated MWNT in the micron scale.

DYNAMIC MECHANICAL PROPERTY BY DMA

Figure 6 shows the storage modulus (G′), loss modulus (G″) and tan δ as a function of frequency for a typical response of PTFE-blended PPS with MWNT nanocomposites. The storage modulus decreased with increasing concentration of MWNT, while maintaining a monotonic behavior in all frequency ranges. The progression of rheological behavior was observed at all frequencies. In addition, the stiffness characteristics of the nanocomposites were investigated by studying the relationship between tan δ and frequency. It was evident that the corresponding curves became flatter with increasing MWNT loading. This behavior was evidence of the presence of an interfacial interaction between PTFE-blended PPS and MWNT.

The interfacial adhesion between PPS matrix and MWNT may be improved through the carboxylic acid group on the surface of functionalized MWNT, which could lead to an efficient load transfer to the nanotube. Compared with conventional thermoplastics, PPS undergoes spontaneous molecular alignment in the melt state due to high rigidity of their chains, which may lead to their excellent physical properties. Therefore, alignment of MWNT with a spontaneous alignment of PPS molecules could give rise to significant enhancement in mechanical properties of PTFE-blended PPS with MWNT nanocomposites. However, MWNT could also prevent the spontaneous molecular alignment of PPS as the

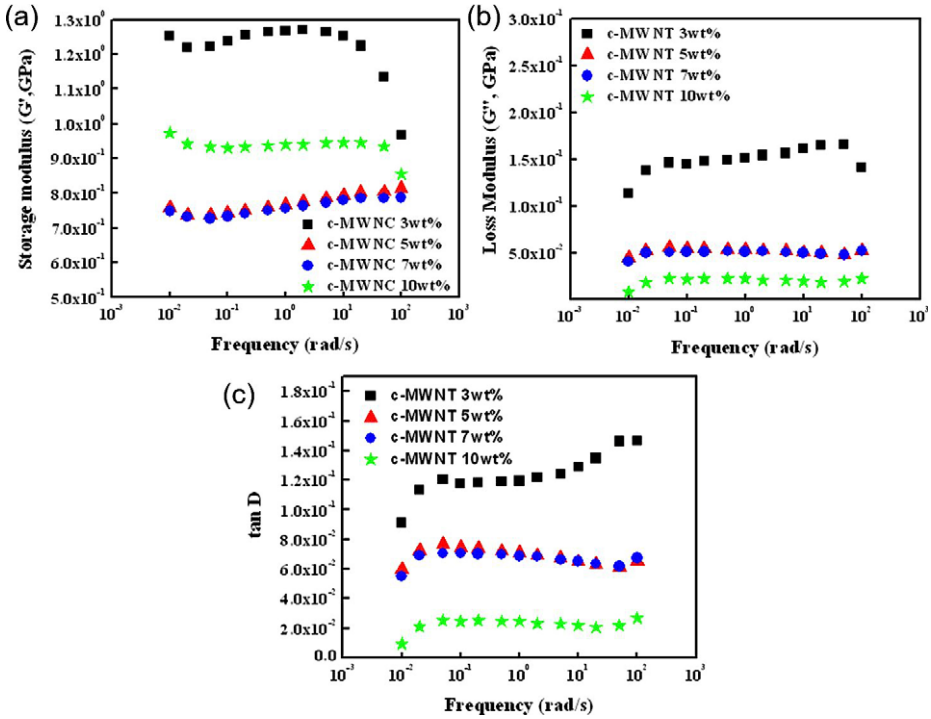

FIGURE 6. (a) Storage modulus, (b) loss modulus, and (c) tan δ versus frequency for PTFE-blended PPS composites with various MWNT loadings.

MWNT content increases, which may lead to the increase in the mechanical properties of nanocomposites.

A well-dispersed MWNT in the polymer matrix is one of the most important and challenging tasks to accomplish. The enhanced performance of the polymer with MWNT nanocomposites results from the homogeneous and uniform dispersion of MWNT, which makes it possible to transfer the load into the nanotube efficiently. Furthermore, the agglomerations of MWNT in the nanocomposites can act as weak points when an external force is imposed upon the nanocomposites; this may be the cause of the stress concentration phenomena.[29] Related work can also be found from other investigators.[4,5,30] As a result, mechanical properties were not improved in higher concentration of MWNT in the nanocomposites because of the presence of some agglomerated structures. In addition, it should be noted that the storage modulus shows a different trend from the loss modulus. This needs to be investigated for further clarification.

Conclusions

In this study, the surface properties of metal were effectively modified to reduce biofouling. The incorporation of CNT into a polymer matrix resulted in the creation of micro/nano structures and superhydrohobic surfaces. Well-dispersed MWNT played an important role in producing homogeneous surfaces in addition to multi-tier micro/nano structures. PTFE nanoparticles incorporated into the PPS matrix resulted in enhanced physical properties of the composites. The morphology of the nanocomposites changed from smooth to nano-pin-like with the addition of small amounts of MWNT. Surfactants played an important role in the growth mechanism of PPS with MWNT. The incorporation of increasing amounts of MWNT in the primary structure led to an increase in the surface roughness, which in turn produced surfaces of varying hydrophobicity. In summary, the mechanical properties of the polymer composites were enhanced by the inclusion of MWNT; however, large concentrations of MWNT in the polymer matrix were detrimental to mechanical properties. Further studies are need to be carried out to evaluate the effects of MWNT in PPS matrixes.

Acknowledgments

The authors thank the U.S. Department of Energy via National Renewable Research Laboratory (NREL) for their financial support (NXL-9-88328-01).

References

1. Townsin, R. L. Biofouling 2003, 19, 9–15.
2. Santos, O.; Nylander, T.; Rosmaninho, R.; Rizzo, G.; Yiantsios, S.; Andritsos, N.; Karabelas, A.; Müller-Steinhagen, H.; Melo, L.; Boulangé-Petermann, L.; Gabet, C.; Braem, A.; Trägårdh, C.; Paulsson, M. J Food Eng 2004, 64, 63–79.
3. Sugama, T. Polym Polym Compos 1998, 6, 373–385.
4. Sugama, T. Mater Lett 2006, 60, 2700–2706.
5. Sugama, T.; Butcher, T.; Ecker, L. Materials Challenges in Alternative and Renewable Energy, Ceramic Transactions; **Wicks, G.; Simon, J.; Zidan, R.; Lara-Cuzio, E.; Adams, T.; Zayas, J.; Karkamkar, A.; Sinderlar, R.; G.-D., B** (Eds.); Wiley: New Jersey, 2010; Vol. 224, pp. 389–401.
6. Massey, L. K. The Effect of Sterilization Methods on Plastics and Elastomers; William Andrew: Norwich, NY, 2005.
7. Saleh, T. A.; Gupta, V. K. J Colloid Interface Sci 2011, 362, 337–344.
8. Mahmoodian, H.; Moradi, O.; Shariatzadeha, B.; Salehf, T. A.; Tyagi, I.; Maity, A.; Asif, M.; Gupta, V. K. J Mol Liq 2015, 202, 189–198.
9. Gupta, V. K.; Saleh, T. A. Environ Sci Pollut Res 2013, 20, 2828–2843.
10. Gupta, V. K.; Agarwal, S.; Saleh, T. A. Water Res 2011, 45, 2207–2212.
11. Saleh, T. A.; Gupta, V. K. Environ Sci Pollut Res 2011, 19, 1224–1228.
12. Gupta, V. K.; Agarwal, S.; Saleh, T. A. J Hazard Mater 2011, 185, 17–23.
13. De Vivo, B.; Lamberti, P.; Tucci, V.; Guadagno, L.; Vertuccio, L.; Vittoria, V.; Sorrentino, A. Adv Polym Tech 2012, 31, 205–218.
14. Szleifer, I.; Yerushalmi-Rozen, R. Polymer 2005, 46, 7803–7818.
15. Yang, M.; Koutsos, V.; Zaiser, M. J Phys Chem B 2005, 109, 10009–10014.
16. Pitalsky, Z.; Tasis, D.; Papagelis, K.; Galiotis, C. Prog Polym Sci 2010, 35, 357–401.
17. Siengchin, S.; Karger-Kocsis, J. J Reinf Plast Compos 2012, 31, 145–152.
18. Tanoue, S.; Hasook, A.; Iemoto, Y.; Unryu, T. Polym Compos 2006, 27, 256–263.
19. Yang, J.; Xu, T.; Lu, A.; Zhang, Q.; Tan, H.; Fu, Q. Compos Sci Technol 2009, 69, 147–153.
20. Saleh, T. A. Appl Surf Sci 2011, 257, 7746–7751.
21. Saleh, T. A.; Agarwal, S.; Gupta, V. K. Appl Catal B 2011, 106, 46–53.
22. Wang, L.; Hu, P.; Tirelli, N. Polymer 2009, 50, 2863–2873.
23. Kubota, S.; Maruyama, T.; Nishikiori, H.; Tanaka, N.; Endo, M.; Fujii, T. Chem Lett 2009, 38, 890–891.
24. Sun, T.; Feng, L.; Gao, X.; Jiang, L. Acc Chem Res 2005, 38, 644–652.
25. Patankar, N. A. Langmuir 2004, 20, 8209–8213.
26. Lee, Y.; Park, S. H.; Kim, K. B.; Lee, J. K. Adv Mater 2007, 19, 2330–2335.
27. Kim, J. Y.; Park, H. S.; Kim, S. H. Polymer 2006, 47, 1379–1389.
28. Butzbach, G. D.; Wendorff, J. H.; Zimmermann, H. J. Die Makromol Chem-Rapid 1985, 6, 821–827.
29. Kim, J. Y.; Kim, S. H. J Polym Sci Pol Phys 2006, 44, 1062–1071.
30. Wu, D.; Wu, L.; Zhou, W.; Yang, T.; Zhang, M. Polym Eng Sci 2009, 49, 1727–1735.